Indian Journal of Advances in Chemical Science

Article

Saraca asoca Leaf Powder as a Biomass-based Adsorbent for Removal of Methylene Blue in Water

Jahnabi Deka[1], Hitesh Das[2], Arundhuti Devi[3], Krishna G Bhattacharyya[4]

[1]Department of Chemistry, Gauhati University, Guwahati, Assam, India, [2]Department of Chemistry, M C College, Barpeta, Assam, India, [3]Institute of Advanced Study in Science and Technology, Guwahati, Assam, India, [4]Department of Chemistry, Assam Don Bosco University, Sonapur, Assam, India

ABSTRACT

Many of the dyes are carcinogenic in nature and their existence in the aquatic system prevents normal biochemical reactions occurring in living systems creating a major problem for the environment. Dyes impart color, which is esthetically unacceptable, and reduces sunlight penetration into natural water. Among the techniques for the removal of dyes from water, adsorption on a suitable adsorbent is a low cost and environment friendly process. In the present study, water spiked with the common dye, methylene blue, has been interacted with *Saraca asoca* leaf powder (SALP), a low cost, locally available biomaterial as an adsorbent. The batch adsorption process was carried out with pH, initial concentration of dye, adsorbent loading, and temperature as the variables. The adsorbent material was characterized with scanning electron microscopy, energy dispersive X-ray, Fourier-transform infrared, CHNS, zeta potential, thermogravimetric analyzer, atomic absorption spectrophotometer measurements and a number of physical parameters such as bulk density, and moisture content were also determined. Adsorption kinetics was tested with Lagergren pseudo-first order, Ho's pseudo-second order, and intra-particle diffusion models. Validity of Langmuir, Freundlich, and Temkin isotherm models were tested with the adsorption equilibrium data to work out the adsorption capacities. The batch adsorption under appropriate conditions can remove the dye from water from 82 to 96%. Langmuir adsorption capacity had the values of 30–125 mg g^{-1}. These results along with the thermodynamic measurements indicated SALP to be a promising adsorption for removal of the dye, methylene blue from water.

Key words: Saraca asoca leaf powder; Methylene blue in water; Adsorption isotherms; Kinetics; Water treatment.

1. INTRODUCTION

The Ashok tree, *Saraca asoca*, is a plant belonging to Detarioideae subfamily of the legume family. It is an important tree in the cultural traditions of the Indian subcontinent and the adjacent areas. The tree has medicinal values as the leaves of *S. asoca* have been known to contain morphine, quinine, nicotine, flavonoids, tannins, benzene, saponins, terpenoids, polyphenolics, glycosides, and many carbohydrates. The functional groups such as -OH, -C=C-, NH^{2-}, >C=O, -COO-, and -O- are available in the plant leaves. The antioxidant activity of the leaf extracts has been described to be due to the presence of polyphenolics such as gallic acid and ellagic acid [1,2].

The hydrosphere is polluted by natural processes, but more prominently by disposal of effluents from various industries such as tanneries, pulp and paper mills, rubber, textiles, sugar and distillery, fertilizers, refineries, dyes and paints, and organic chemicals as well as discharges from agricultural fields, domestic wastewater, sewage, etc. [3]. Many of the effluents of the industries are highly colored due to the presence of dyes and pigments leading to an increase in the biochemical oxygen demand and chemical oxygen demand, changes in acidity and alkalinity or pH, dissolved solids (ionic and non-ionic), and various toxic components in the aquatic ecosystem [4]. It is reported that 10–25% of dyes are lost during the dyeing process and 2–20% are discharged into the wastewater creating various problems for the environment [5].

Methods such as decomposition, coagulation, reduction-oxidation, precipitation, ion-exchange, reverse osmosis, and adsorption have been in use to remove the pollutants from water. Among these methods, adsorption on a suitable adsorbent has been recognized as highly cost effective, less troublesome, and environment friendly [6]. The use of activated carbon for removal of dyes from water is a common practice but production and regeneration of the carbon require high cost and there has been a demand for use of cheap biomaterials as adsorbents making the process of dye-removal very cost-competitive [7,8]. Many low-cost biomaterials such as banana pseudo-stem fiber, orange peel, ginger waste, garlic peel, neem leaves, coir pith, mango seed kernel powder, papaya seeds, carbonized saw dust, and coffee husk have been under test as effective bio adsorbent for removal of dyes from water [9-11].

In the present work, the use of Ashoka tree (*S. asoca*) leaf powder to remove methylene blue from water is reported. The dye, methylene blue is a heterocyclic aromatic chemical compound with a molecular formula $C_{16}H_{18}N_3SCl$ [3, 7-bis (dimethylamino)-phenothiazine-5-ium chloride] used in leather and garment industry [12]. It can cause

***Corresponding author:**
E-mail:kgbhttacharyya@gmail.com

ISSN NO: 2320-0898 (p); 2320-0928 (e)
DOI: 10.22607/IJACS.2021.901001

Received: 02nd November 2020;
Revised: 05th December 2020;
Accepted: 09th December 2020

many disorders such as nausea, vomiting, and diarrhea and it is also allergic to the skin when in contact [13]. Batch adsorption studies were carried out to evaluate *S. asoca* leaf powder (SALP) as an effective bio adsorbent for the dye, methylene blue, in water under various experimental conditions.

2. MATERIALS AND METHODS

2.1. Materials

Methylene blue (basic blue 9, C.I. 52015; chemical formula, $C_{16}H_{18}N_3SCl$, MW, 319.85 g/mol) was used as a model cationic dye for the adsorption process. Methylene blue (Merck Mumbai) HCI (Merck Mumbai) and NaOH (Merck Mumbai) were purchased from a local supplier and were used as received without further purification.

2.2. Preparation of Adsorbent

The matured leaves of Ashoka (*S. asoca*) were collected from the district, Barpeta in Assam, India. The leaves were washed several times with water to remove dust and other soluble materials and were allowed to dry at room temperature for several days. The clean leaves were kept in an air oven at 105°C till they became very crisp and were then ground in an electric grinder to obtain a fine powder. The powder was dispersed in distilled water to remove pigments and soluble materials from it, separated by filtration/centrifugation, dried again at ~105°C. The powder was sieved through several sieves and the fractions retained between 63 and 125 μ were kept for use as the bio adsorbent, stored in airtight plastic bottles in a laboratory refrigerator.

2.3. Preparation of Dye Solutions

Methylene blue stock solution of concentration, 1000 mgL^{-1}, was prepared by dissolving an accurately weighed amount of the dye in double distilled water. The stock solution was diluted with appropriate volumes of double-distilled water to obtain dye solutions of concentration, 5, 10, 15, 20, 25, and 30 mg L^{-1}. The pH of the dye solution was maintained at the desired value by adding 0.1 M NaOH or HCl solution in drops. The structure of methylene blue is shown in Figure 1.

2.4. Characterization of the Adsorbent

Fourier transform infrared (FTIR) spectroscopy (Model: Perkin-Elmer FTIR spectrometer, range 4400–400 cm^{-1}) with a resolution of 4 $cm^{-1}$was used to investigate the surface functional groups of the adsorbent, SALP, using 150 mg KBr disks containing approximately 2% of the adsorbent. The ζ -Potential measurements related to the charge and electric double layer of surfaces in aqueous solutions of the adsorbent were carried out with a micro electrophoretic zeta potential analyzer at 295–301 K at Institute of Advanced Study in Science and Technology (IASST), Guwahati. The elemental identification (Scanning Electron Microscopy [SEM]/Energy Dispersive X-ray [EDX]) was carried out Zeiss SEM, Sigma VP, with EDAX at Gauhati University [14]. EDX analysis was used to determine the elemental composition of individual points or to map out the lateral distribution of elements from the imaged area of the adsorbent [15,16]. The adsorbent was examined for the presence of metals such as Na, K, Ca, Mg, Fe, Cu, Zn, and Mn by Atomic Absorption Spectrophotometer (AAS) (VARIAN SpectrAA 220). Euro EA elemental analyzer at the IIT Guwahati was used for elemental analysis of the adsorbent as per linear and configuration CHNS [17]. Evaluation of the thermal behavior of the material was studied with Thermo Gravimetric Analyzer (Perkin Elmer, USA) over the temperature range of 0–1000°C. The physicochemical properties such as moisture content, ash content, and organic matter content for the adsorbent were measured in accordance to standard procedures [18,19].

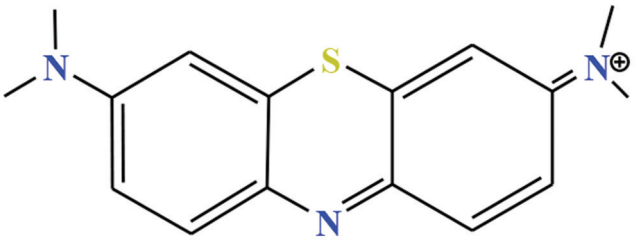

Figure 1: Structure of the dye, methylene blue.

2.5. Adsorption Measurements

The effects of pH (2.0, 4.0, 6.0, 8.0, 10.0, and 12.0) were studied by adjusting the pH of methylene blue dye solutions using 0.1 N HCl and 0.1 N NaOH solutions. The pH was measured for a solution of methylene blue (300 mg/L) using a glass-electrode digital pH meter (PHS-3B PHTEK), previously set with buffer solutions at pH of 4 and 7. The effects of adsorbent loading (0.1–0.8 g) were evaluated by interacting with 200 ml of methylene blue solution of initial concentration 100 mg/L (contact time 120 min). 200 mL solutions of methylene blue dye with different initial concentration (5, 10, 15, 20, 25, and 30 mg/L) were used to obtain the adsorption characteristic of the adsorbent under different dye concentrations.

The batch adsorption studies were carried out at different adsorbent loadings, pH, initial dye concentration, and contact time. For each experimental run, 200 ml of dye solution of known concentration was taken in a 250-mL plastic Erlenmeyer flask and was agitated with a known amount of adsorbent at room temperature (25 ± 2°C) using a shaker at constant oscillation of 350 osc/min for a desired period of time. At the end of adsorption test, samples were centrifuged and the concentration of residual dye in the supernatant solution was analyzed using a UV/VIS spectrophotometer (Shimadzu 1800, Singapore) by monitoring the absorbance at a maximum wavelength (λ_{max}) of 662 nm. Blank experiments with only the adsorbent in 200 ml of distilled water were conducted simultaneously at the identical conditions to account for any color leached by the adsorbent and adsorbed by glass containers.

2.6. Calculations

The Langmuir, Freundlich and Temkin isotherms, applied to the adsorption data, are:

$$\text{Langmuir Isotherm: } C_e/(x/m) = (1/KV_m)+(C_e/V_m) \quad (1)$$

where C_e is the equilibrium concentration of the dye solution, x/m is the amount adsorbed per unit mass of the bio adsorbent, m is the mass of the bio adsorbent, V_m is the monolayer capacity (maximum adsorption capacity), and K is an equilibrium constant, related to the heat of adsorption, q or the energy of adsorption by the equation

$$K = K_0 \exp(q/RT) \quad (2)$$

where q is the heat of adsorption. Linear Langmuir plots from Eq. (1) were used to compute the values, Vm and K.

$$\text{Freundlich Isotherm: } x/m = K_f C_e^{1/n} \quad (3)$$

or,

$$\log x/m = \log K_f + (1/n) \log C_e \quad (4)$$

where K_f is the measure of adsorption capacity, $1/n$ is adsorption intensity and other parameters have been defined as in Eq. (1). Plot of

log (x/m) against log C_e gives a straight line, the slope and intercept of which correspond to 1/*n* and log K_f, respectively.

The linearized form of the Langmuir equation is:

$$C_e/q_e = 1/q_m\, b + C_e/q_m \quad (5)$$

where b (L/mg) is the Langmuir adsorption constant and q_m (mg/g) is the maximum amount of adsorption corresponding to complete monolayer coverage on the surface, q_e (mg/g) is the amount of dye adsorbed at equilibrium, and C_e (mg/L) is the equilibrium concentration of dye in solution. The dimensionless constant separation factor (R_L) is calculated using the equation:

$$R_L = 1/(1+bq_m) \quad (6)$$

The nature of the adsorption process can be described on the basis of R_L as unfavorable ($R_L > 1$), linear ($R_L = 1$), favorable ($0 < R_L < 1$), and irreversible ($R_L = 0$).

The linearized Freundlich equation is as follows:

$$\log q_e = \log K_F + 1/n \log C_e \quad (7)$$

where K_F is an indicator of adsorption capacity (mg/g) and 1/*n* is the adsorption intensity.

Temkin isotherm model takes into account the effects of indirect adsorbent/adsorbate interactions on the adsorption process; it is also assumed that the heat of adsorption, ΔH_{ads}, of all molecules in an adsorbed layer decreases linearly as a result of increased surface coverage. The Temkin isotherm is valid only for an intermediate range of ion concentrations. The linear form of Temkin isotherm is given by

$$q_e = \frac{Rt}{b}\ln Kt + \frac{Rt}{b}\ln C \quad (8)$$

where b is Temkin constant, related to the heat of sorption (J mol^{-1}) and K_t is Temkin isotherm constant (L g^{-1}).

The kinetics of the adsorption processes was studied by carrying out a separate batch of experiments at constant temperature with a fixed ASLP amount and a fixed dye concentration, using pseudo-first-order kinetics, pseudo-second-order kinetics, and Weber and Morris's intra-particle diffusion model. The Lagergren pseudo-first-order kinetic equation is

$$\log (q_e - q_t) = \log (q_e) - k_1 t/2.303 \quad (9)$$

where q_e and q_t refer to the amount of dye adsorbed (mg g^{-1}) at equilibrium and at any time t (min), respectively, and $k_1$is the equilibrium rate constant of pseudo-first-order adsorption (min^{-1}). The pseudo-second-order kinetics was tested with the equation

$$t/q_t = 1/k_2 q_e^2 + t/q_e \quad (10)$$

where $k_2$is the equilibrium rate constant of pseudo-second-order adsorption (g $mg^{-1} min^{-1}$). The intra-particle diffusion model, employed to identify if the dye adsorption follows a diffusion mechanism by obtaining q_t versus $t^{1/2}$ curves from the equation

$$q_t = k_p\, t^{0.5} + c \quad (11)$$

where c is the intercept and k_p is the intra-particle diffusion rate constant (mg g^{-1} $min^{-0.5}$), obtained from the slope of the q_t versus $t^{1/2}$straight lines.

The thermodynamic parameters, that is, standard Gibbs' free-energy change (ΔG^0), standard enthalpy change (ΔH^0), and standard entropy change (ΔS^0), are important since they determine the spontaneity of a given sorption process. These parameters are obtained from the well-known relationships (Thomas and Crittenden 1998), namely,

$$\Delta G^0 = -RT \ln K_a \quad (12)$$

$$\Delta G^0 = \Delta H^0 - T\Delta S^0 \quad (13)$$

$$\log q_e/C_e = \Delta S^0/2.303R - \Delta H^0/2.303RT \quad (14)$$

where $K_a = q_e/C_e$ is known as the adsorption affinity. The values of ΔS^0 and ΔH^0 could be obtained from the plots of log (qe/Ce) versus 1/T.

3. RESULTS AND DISCUSSION

3.1. Characterization of SALP

The leaves of *S. asoca* contain various ionizable functional groups, which are confirmed by the FTIR spectroscopy shown in Figure 2. The presence of ionizable functional groups in the bio material favors the adsorption of dyes [20,21]. The peaks observed in the spectrum at 3245–3250 cm^{-1} and 1665–1680 cm^{-1} suggest the presence of –OH and C=O groups [22]. These functional groups interact with the cationic dye, methylene blue during adsorption. Moreover, the peaks at 2960–2800 cm^{-1} indicate the presence of saturated methylene; methyl and methine groups in the adsorbent. The broad band of stretching vibration of O-H group is located at 3446 cm^{-1}. This peak indicates the presence of molecular H_2O. The peak at 2924 cm^{-1} indicated the presence of stretching C-H bond in methyl group in the adsorbent [4]. The peak located at 1736 cm^{-1} is also due to characteristic carbonyl (C=O) group stretching [4]. The lignin structure of *S. asoca* can be confirmed for having a peak at 1052 cm^{-1} in the spectra. The peaks in the range of 900–1300 cm^{-1} are the result of the stretching vibration of C-O of phenols, ethers, esters or alcohols present in the bioadsorbent. The peaks around the vibrations at 1450–1470 cm^{-1} are considered due to the presence of aliphatic and aromatic (C-H) groups in methyl, methylene, and methoxy groups [23]. Some bands are closely appeared at 1750 cm^{-1} and 1100 cm^{-1} were attributed to carboxylic groups predominantly [24]. The FTIR of *S. asoca* showed very closely packed spectral lines around 2341 cm^{-1} indicate the presence of C-H stretching which are very similar to lignocellulosic plants and the peaks at 787–706 cm^{-1} of raw *S. asoca* are considered to CH_2 rocking [25]. Therefore, the FTIR reveals that the bioadsorbent has hydroxyl, carbonyl, and ionizable carboxyl groups for which the cationic dye can be easily adsorbed on these adsorption sites [22].

In the FTIR spectra that obtained for the lignin type of compound, a peak at 1029.87 cm^{-1} reported for the bending vibration of -OH and

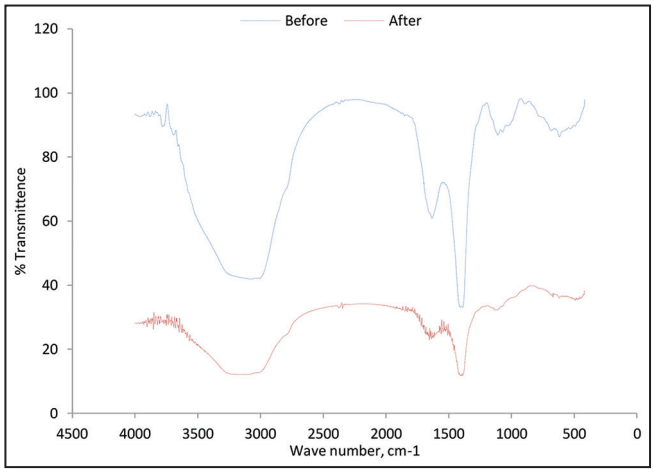

Figure 2: Fourier-transform infrared spectra of *Saraca asoca* leaf powder before and after adsorption of the dye, methylene blue.

stretch vibration of C-O-C. The same peak is obtained in our adsorbent *S. asoca* and hence these functional groups are active sites for the removal of cationic dyes [26].

The overall FTIR spectra of all three adsorbents that selected for present study provided the information for the presence of cellulose; hemicelluloses and lignin type of compounds were in the adsorbents. Furthermore, the spectra revealed the character related to chemical nature and properties of these substances were not changed after pretreatment and surface modification. This type of results is also reported by other authors [27].

The zeta potential measurements showed that the surface of *S. asoca* powder particles is negatively charged from pH 5.0–10.0 (Figure 3). The zeta potential depends on pH and ion concentration of the surface charge of the particle as well as on the environmental conditions. The zeta potentials were calculated for all the adsorbents as shown in the Figure 3 from the electrophoretic mobilities by following the equation of Smoluchowski [28]. Thus, the methylene blue cations would have favorable adsorption at this pH-range on the negatively charged adsorbent surface. The point of zero charge or the isoelectronic point of the SALP was found at pH around 5. Therefore, adsorption of methylene blue dye particles will be accumulated over potential 2.1 mV [29]. Thus, the dye uptake capacity of SALP will be high at higher pH [30,31].

The surface-topographical analysis of SALP (Figure 4a and b) shows that the morphology was characterized by a high degree of roughness, waviness, porous, and finely segregated particles. These porous and irregular surfaces are thought to be very useful in adsorbing the dye cations. The EDX images (Figure 4c and d) further support the occurrence of dye adsorption on the adsorbent surface. The well-defined peak of adsorbent loaded with methylene blue dye showed that the dye was bound onto the adsorbent surface. The peaks after adsorption were very small suggesting that the dye cations were held on the adsorbent surface by weak forces [32].

Due to the presence of pores on the surface (Figure 4), the adsorbent could be considered as suitable for holding the large methylene blue cations. The cavities on the surface are not smooth and could be considered as channels instead of pores. In addition, the surface of SALP could also be considered as composed of multiple layers of thin films that may be useful in capturing the dye molecules or ions. Figure 4b shows that after adsorption, the SALP surface became smooth with less visible pores, indicating covering of the pores and channels with the dye [33,34].

The phase contrast micrographs or microscopy image (Figure 5a and b) confirm SALP as a grouping of fine particles of lopsided shape and size. The particles having very rough porous surface before adsorption are prone to play a significant role as potential active sites for adsorption. The electron microscope image after adsorption of the dye clearly shows

The phase contrast microscope that used for the analysis is the phase contrast microscope manufactured by Nikon, available in IASST, Boragaon, Guwahati (Assam). The plane surface of adsorbent free from any pores and roughness that viewed with an electron microscope can provide best image of that adsorbent with the adsorbate after the adsorption with the help of contrast phase microscope. The image can be analyzed for the adsorbent before and after the adsorption of dye. The image of phase contrast microscopic images supports the adsorption of methylene blue in lopsided shape and sizes of the *S. asoca* leave powder photographs.

The adsorption process depends on the physicochemical properties such as carbon yield, ash content, and moisture content of the selected adsorbent. SALP has low ash content and high yield of carbon content indicating its purity and a high adsorption affinity towards the dye. The present study on *S. asoca* shows (Table 1) low ash content signifies a good adsorbent for the removal of dye particles. High presence of ash or inorganic matter which is chiefly of earthy mineral particles is undesirable for activated carbon since it reduces the mechanical strength of carbon and affects adsorptive capacity [34,35].

The physicochemical properties moisture content (%), ash content (%), volatile matter (%), and fixed carbon (%) as shown in Table 1 are determined gravimetrically. The known amount of *S. asoca* leave powder adsorbent (2 g) is placed in a dry silica crucible of weight W_1 and the weight of the crucible with adsorbent will be W_2, $W_2 > W_1$. The crucible with the adsorbent is kept into the hot air oven at 388 K for 16 h. The crucible is then measured for the final weight W_3 and the weight (%) of the dried sample is measured for the moisture content in the adsorbent using the relationship in Equation 15.

$$\text{Moisture content } (\%) = \frac{W_2 - W_3}{W_2 - W_1} \times 100 \quad (15)$$

where $(W_2\text{-}W_3)$ is the weight of evaporated water, $(W_2\text{-}W_1)$ the oven dry weight of the adsorbent.

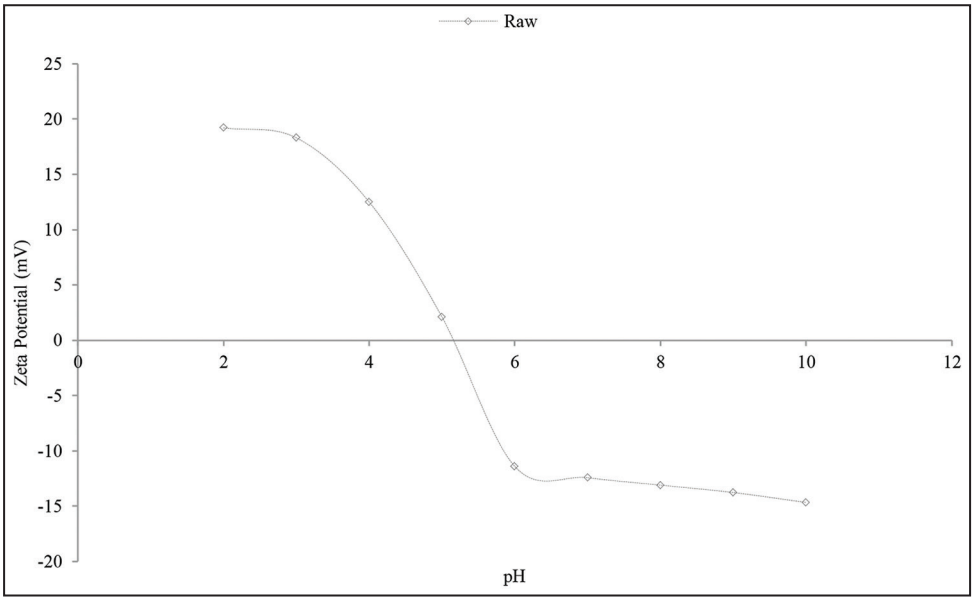

Figure 3: Variation of the zeta potential of *Saraca asoca* leaf powder with pH.

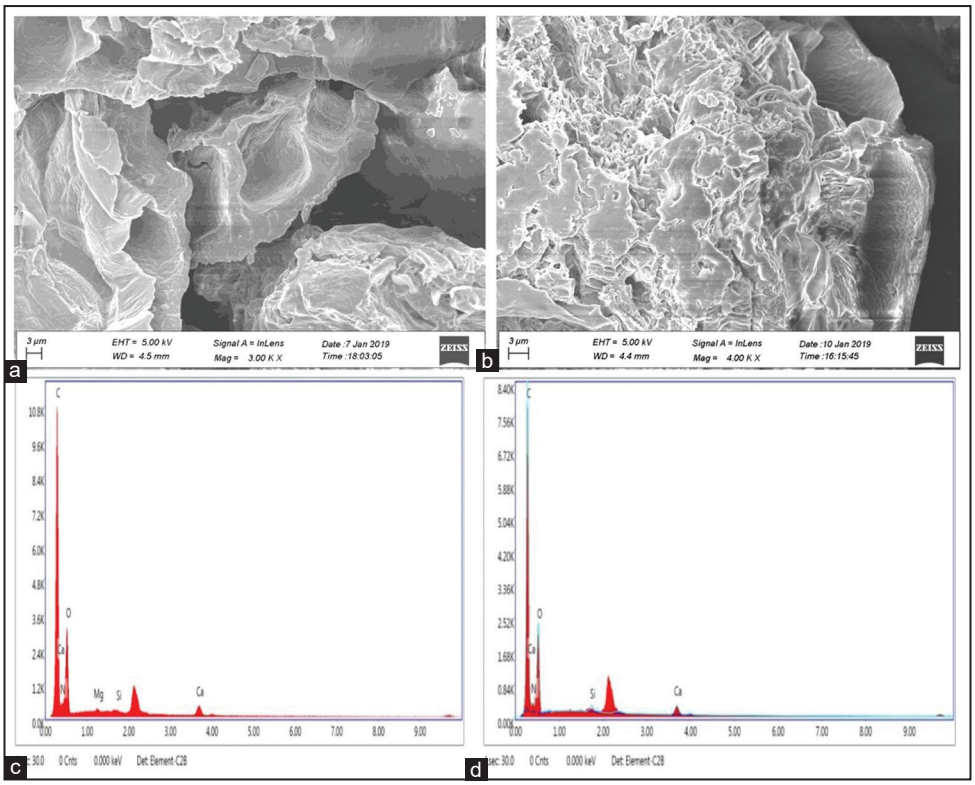

Figure 4: Scanning electron microscopy images of *Saraca asoca* leaf powder before (a) and after adsorption (b) of the dye along with energy dispersive X-ray patterns, before (c) and after adsorption (d). covering of the pores with the dye with much reduced roughness.

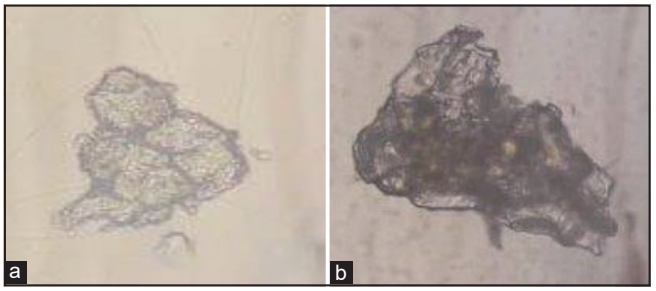

Figure 5: Contrast microscopic images of *Saraca asoca* leaf powder before adsorption (a) and after adsorption of the dye (b).

Table 1: Physicochemical properties of *Saraca asoca* leaf powder along with element analysis (proximate and ultimate content).

Proximate content (in %)		Ultimate content (%)	
Moisture content	5.86	Carbon	56.6
Ash content	12.9	Nitrogen	2.47
Volatile matter	37.24	Sulfur	3.9
Fixed carbon	56		

Ash content of the adsorbent sample was determined by placing a marked 50 cm^3 ashing porcelain crucible in a muffle furnace at 873 K for a period of 4 h. After ashing, the crucible was cooled for 1 h, then directly transferred from the furnace into desiccator. The weight of the crucible was then measured and recorded to the nearest 0.1 mg as W_a. The 4 g of adsorbent, oven-dried at 388 K and stored in desiccators, was weighed into the ashed crucible and initial weight of crucible with sample recorded as W_b; and then introduced into the muffle furnace and ashed at 873 K for 4 h to a constant weight (change of <±0.3 mg) and final weight of crucible with sample recorded as W_c. The percentage ash content was calculated using Equation 16.

$$\text{Ash content } (\%) = \frac{W_b - W_c}{W_b - W_a} \times 100 \quad (16)$$

where (W_b-W_c) is the weight of the ashed sample without the crucible and (W_b-W_a) the weight of the oven dried sample without the crucible.

The volatile matter contents of the adsorbents were determined from the difference between 100% oven dried adsorbent and the percentage ash contents as illustrated in Equation 17.

$$\text{Volatile matter content } (\%) = 100 - \%\ \text{Ash content} \quad (17)$$

$$\text{Fixed carbon (FC)}\% = 100 - (\text{moisture content } \% + \text{volatile matter } \% + \text{ash content } \%) \quad (18)$$

Moreover, the equipment called Euro EA elemental analyzer available in Biotech Park of Indian Institute Technology, Guwahati (IITG) was applied for CHNS analysis for bioadsorbents as per standard procedures. In this process, the bioadsorbent undergoes combustion at high temperature (1273 K) in an oxygen rich environment or tools. As a result, carbon is converted into carbon dioxide, hydrogen to water, nitrogen to nitrogen gas or oxides of nitrogen and sulfur to sulfur dioxide. The results are displayed in Table 1.

The fixed carbon content indicates the percentage of carbon remaining after subtracting the proportion of moisture, ash, and volatiles. The ash content plays an important role in the adsorption of dye from its solution when it is present in small amounts. The experimental results showed that the ash content of SALP was as low as 12.9%.

Furthermore, the contents of sulfur and nitrogen were low at 3.9% and 2.47%, respectively. Therefore, nitrogen and sulfur based functional groups are not expected to affect the adsorption of methylene blue by SALP [36]. The literature of other researchers has cited the low ash content and low moisture is an indicative property for a suitable adsorbent for the removal of dyes [37]. The elemental composition of SALP (Table 2) shows the presence of Fe, Zn, Mn, Mg, K, Cu, and Na in appreciable quantities; however, they are unlikely to play any significant role in adsorption of the methylene blue cations [37]. The elements are determined by the AAS spectroscopy after following the standard procedure. The 100 mg of dried ash sample that obtained after following the equation (16) is placed to a crucible and the ash content crucible is kept inside muffle furnace at the temperature 873K for about 48 h till the sample becomes white completely. The crucible is allowed to cool down inside the furnace. The cooled white ashed sample is kept inside the dessicator for having moisture free. The ash sample is mixed with 10 mL of 2N HNO_3 and the resultant solution is through a filter paper (Whatman No. 42) and it is transferred into a volumetric flask of 50 mL. The volume of the filtrate is made up to 50-ml using double distilled water [38,39]. The determined values of trace elements such as potassium, magnesium, zinc, copper, manganese, and sodium are given in Table 2.

The thermogravimetric analysis of SALP (Figure 6) shows the thermal stability of the adsorbent under inert or oxidizing conditions.

The thermogram of SALP; (Figure 6) shows the weight loss with increasing temperature in several steps. These are: (i) No loss in weight up to 329.7 K, (ii) a weight loss of 4–5% from 333 to 383 K due to loss of moisture content, (iii) a minor weight loss up to 466K, indicating the thermal stability of SALP, (iv) a sharp 48% weight loss from 466 to 687K due to decomposition of different components in the adsorbent,

Table 2: Elemental composition of *Saraca asoca* leaf powder (mean±SE).

Element	mg/kg
Fe	52.02±0.11
Zn	316.18±1.04
Mn	83.79±0.04
Mg	179.21±2.25
K	67.82±0.03
Cu	35.40±0.23
Na	43.98±0.26

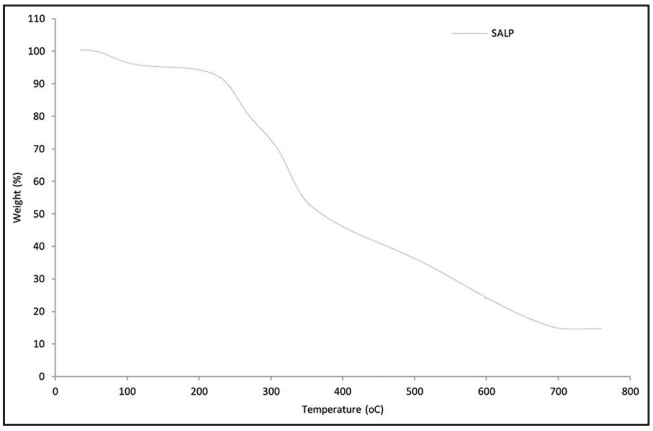

Figure 6: Thermogravimetric analyzer graph of *Saraca asoca* leaf powder.

(v) a weight loss of 33% from 687 to 853K, suggesting almost complete decomposition of the residual constituents of the adsorbent, and (vi) a loss of about 14.7% corresponding to the ash content present in the biomass up to about 1013 K, [40]. The absence of remarkable constant weight above 1013 K indicates the carbon optimization temperature to be about 1023 K.

3.2. Adsorption

3.2.1. The effect of pH

The adsorption capacity of SALP for methylene blue increases with increase in pH (Figure 7). At lower pH, electrostatic repulsion occurs between the dye cations and H^+ ions on the surface of the adsorbent. These repulsions decrease as the pH increases and as the adsorbent surface gradually turns negative. At pH above 6, there is accumulation of HO^- ions on the adsorbent surface and there would be a preference for the adsorption of methylene blue cations on the adsorbent surface [32,35,41].

Thus,

At acidic medium,

$$\text{Adsorbent-----OH} + H^+ \rightarrow \text{Adsorbent--------OH}^{+2}$$

$$\text{Adsorbent-----COOH} + H^+ \rightarrow \text{Adsorbent-----COOH}^{+2}$$

At basic medium, (deprotonation at higher pH)

$$\text{Adsorbent ------OH} + OH^- \rightarrow \text{Adsorbent ---- } {-}O{-} + H_2O$$

$$\text{Adsorbent ------ COOH} + OH^- \rightarrow \text{Adsorbent -----COO}^- + H_2O$$

From pH 2 to 4, the removal of the dye from the aqueous phase was recorded from 15 to 76.5% and at pH 6 to 12, the removal efficiency increased from 91 to 93.5% (Figure 7).

3.2.2. The effects of adsorbent loading and adsorbate concentration

The effects of adsorbent dose for a particular adsorbent play an important role in the removal of colored adsorbates for its given initial concentrations (Sari *et al*., 2007). With the variation of adsorbate-adsorbent concentration, the effect of adsorbent dose played an important role for the adsorption of cationic dye, methylene blue. The dye removal decreased for a fixed adsorbate concentration as shown in Figure 8. However, the amount of methylene blue adsorption increased with increasing concentration of adsorbate from 5 to 30 mg/L as shown in Figure 8. The adsorption started with more adsorption for each adsorbate concentration but with the increase in the amount of adsorbent declined as shown in Figure 8 and a similar trend was observed by the other author [42].

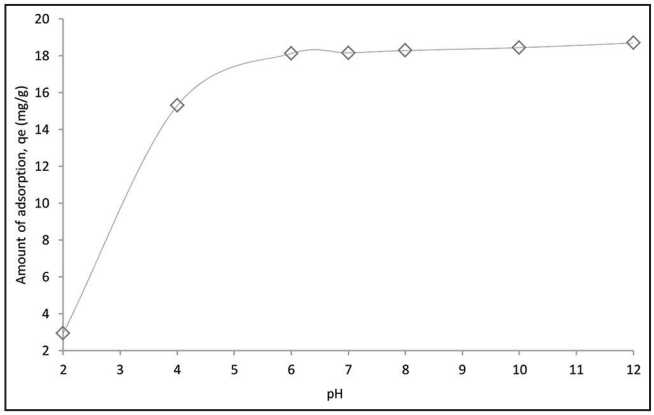

Figure 7: The extent of adsorption of methylene blue dye on *Saraca asoca* leaf powder at 303 K (Dye 50 mg/L, interaction time 120 min).

At lower adsorbent concentration, the number of adsorption sites was higher for which accumulation of dye particles was higher and the uptake capacity decreased with the increase of amount of adsorbent dose [43].

Larger dye uptake of 80.7-95.8% was observed for SALP loadings (0.1–0.7 g/L) for a methylene blue concentration of 30 mg/L was due to increase in the number of adsorption sites as shown in Figure 9. The increase in methylene blue concentration for a fixed adsorbent amount (0.1–0.7 g/L) results in a decline in the dye removal from 95.8 to 71.9% in the Figure 9 as the increasing number of methylene blue cations had to compete for a constant number of available active adsorption sites on the adsorbent surface.

3.2.3. Effects of contact time on removal of dye and adsorption kinetics

For the various initial concentrations of dye solutions, 5–30 mg/L, the percentage removal of methylene blue at 303 K by *S. asoca* (1 g/L) as a function of contact time is illustrated in Figure 10. From the plots, it is evident that for the various initial concentrations of dye, maximum adsorption was achieved in the first 20 min itself with equilibrium being slowly reached in 120 min. For a dye solution of 5 mg/L, 95.9% adsorption was possible in 120 min from where the adsorption equilibrium is started. This quick removal of dye by the adsorbent has indicated the affinity of *S. asoca* for methylene blue [44].

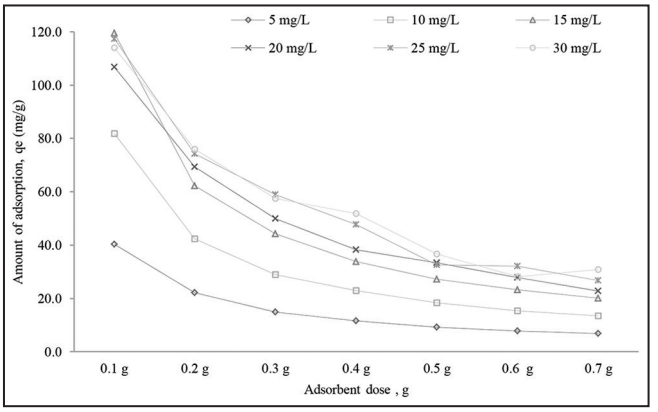

Figure 8: The effects of *Saraca asoca* leaf powder loading (0.1–0.7 g/L) and initial concentration of the methylene blue dye (5–30 mg/L) on dye adsorption at 303 K.

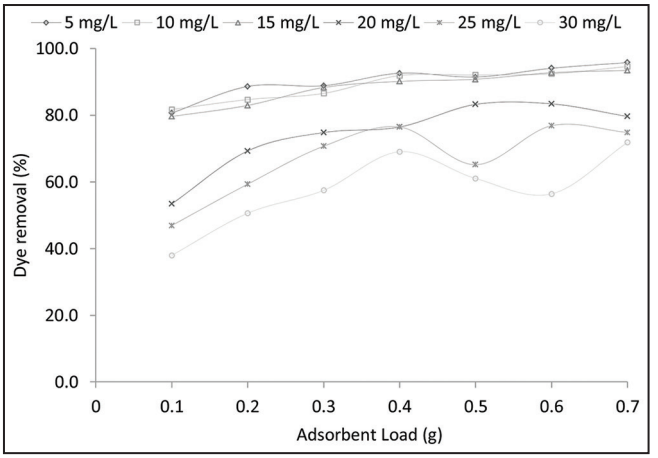

Figure 9: The effects of adsorbent loading and adsorbate concentration on adsorption of methylene blue on *Saraca asoca* leaf powder at 303 K.

The kinetics of the adsorption process was carried out for Lagergren pseudo-first-order kinetics (Figure 11), pseudo-second-order kinetics (Figure 12), and the intra-particle diffusion model (Figure 13) which are displayed below.

The Lagergren plots for the adsorption of dye on the adsorbent, SALP, are of near-perfect straight lines which confirmed that the adsorption mechanism followed pseudo-first-order kinetics with average value of the rate constant of 3.6×10^{-2} min^{-1}. The dye uptake capacity, q_e values

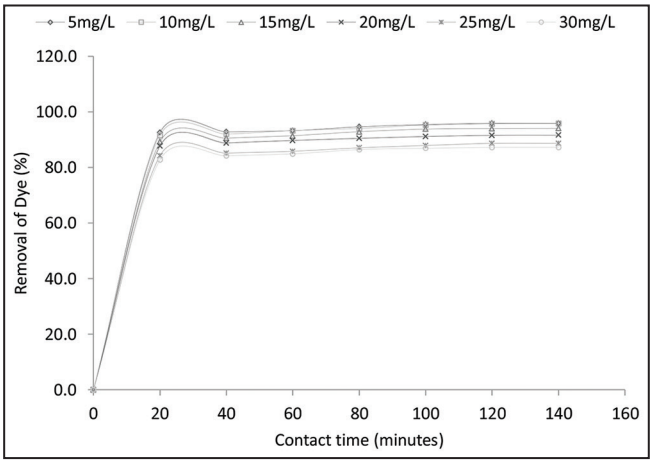

Figure 10: Variation of % removal of dye with time (min) for different dye concentrations 5–30 mg/L using adsorbent 1 g/L at temperature 303 K.

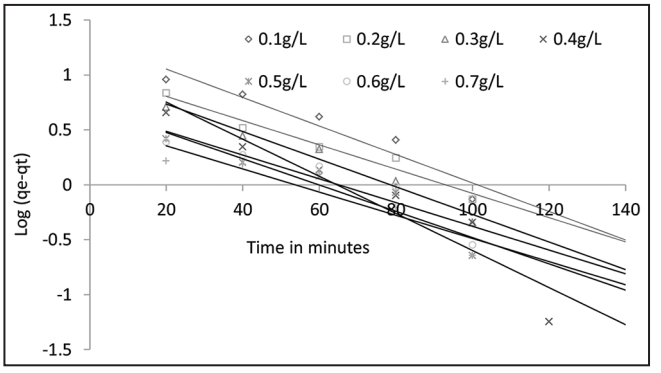

Figure 11: Lagergren's plots for adsorption of methylene blue dye at 303 K on *Saraca asoca* leaf powder (0.1–0.7 g/L) at dye concentration of 5 mg/L.

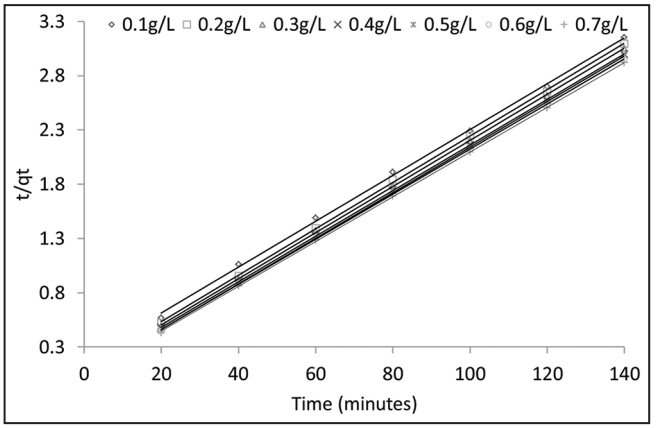

Figure 12: Pseudo-second-order kinetics plots for adsorption of methylene blue dye at 303 K on *Saraca asoca* leaf powder (0.1–0.7 g/L) for the dye concentration of 5 mg/L.

for pseudo-second-order kinetics are high and also the correlation coefficients are almost one. Therefore, the pseudo-second-order model was most likely for the adsorption processes for methylene blue adsorbate and SALP adsorbent, that is, the interactions led to covalent bond formation between them [45-47].

The pseudo-first-order and intraparticle diffusion equations are not found suitable and well defined in terms of the correlation coefficients which are small in comparison to coefficients observed for pseudo-second-order mechanism (Table 3). The plots of q_t versus $t^{0.5}$ (Figure 13) exhibit more than one slope of the straight lines for different adsorbent dose (0.1–0.7 g/L). The intraparticle diffusion might have a significant role as the lines have different slopes and intercepts for the adsorption of dye [48,49]. The different intercepts for these lines suggested that adsorption kinetics for the present study will not be controlled by intraparticle diffusion mechanism [50].

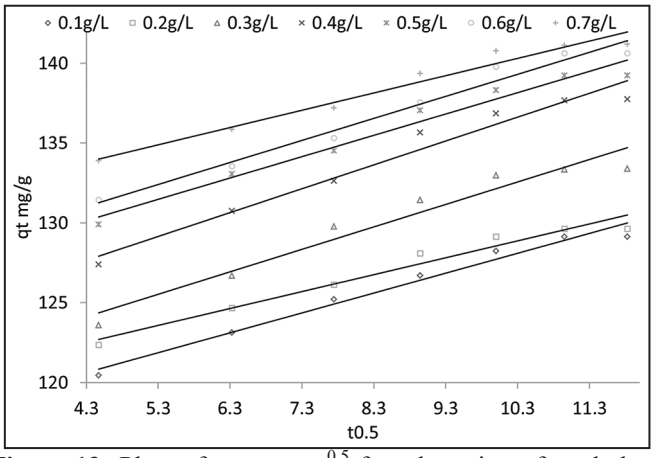

Figure 13: Plots of q_t versus $t^{0.5}$ for adsorption of methylene blue dye (concentration 15 mg L^{-1}) on *Saraca asoca* leaf powder at 303 K.

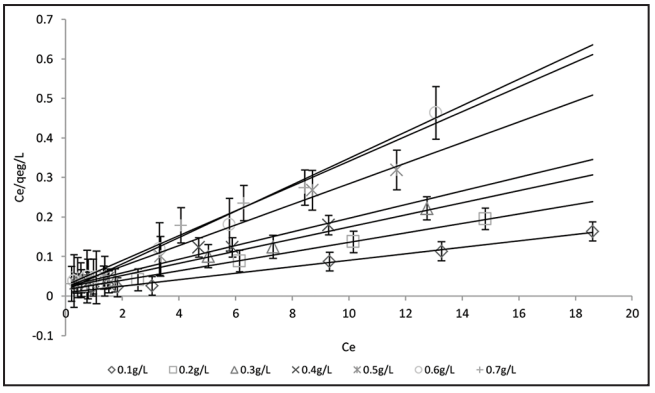

Figure 14: Langmuir isotherm plots for the adsorption of methylene blue (5–30 mg/L) onto *Saraca asoca* leaf powder at 303 K.

The kinetics of adsorption of methylene blue follows pseudo-secondorder mechanism for which the removal of methylene blue was maximum and therefore the average experimental value and theoretical value had a difference of 0.06 mg/g. The theoretical and experimental values are the same for the adsorption of dye (5 mg/L) on the adsorbent (1 g/L).

3.2.4. Adsorption isotherm

The adsorption isotherm is an indication for the adsorbate-adsorbent interactions. The present work on the adsorption of methylene blue on SALP was examined with three isotherm models, Langmuir, Freundlich, and Temkin models. The adsorption isotherms for methylene blue on SALP yielded good fits with Langmuir, Freundlich, and Temkin Isotherm models. The isotherm plots are shown in Figures 14-16. All the experimentally obtained values for the different parameters showed excellent agreement with the theoretical concepts showed in Table 4. Thus, SALP has the potential for removal of the dye in comparison to several other adsorbents [51,52].

The linear regression correlation coefficient, R^2 for the adsorption of the cationic dye, methylene blue onto the adsorbent raw *S. asoca* was in the range of 0.62–0.90. The K_F value was in the range of 15.0–58.6 L/mg which is considerable for a particular adsorbent. The 1/n and n values for SALP were in the range of 0.28–0.42 and 2.4–3.6, respectively. These values confirm the heterogeneity of the adsorbent, raw *S. asoca* and established the unequal distribution of binding energies on accessible active sites on the surface of the adsorbent. Similar type of findings was reported for the adsorption of malachite green on the almond shell bioadsorbent. The Freundlich isotherm fitted well for the adsorption of anionic dyes, malachite green, and Eriochrome black on almond shell bioadsorbent [53].

The Langmuir isotherm model usually describes the equilibrium uptake isotherms of homogeneous surfaces of the bioadsorbents and there is no interaction between the adsorbed dye particles on the surface of adsorbent. The linear regression correlation coefficients (R^2) were from 0.980 to 0.998 indicating that the adsorption isotherm is a best fit with the formation of monolayer over the bioadsorbent. The maximum monolayer capacity was 125.0 mg/g for 0.1 g/L and 32.26 mg/g for 0.7 g/L of *S. asoca* leave powder. The dimensionless parameter, R_L, had values (Table 4) very close to zero suggesting the adsorption process to be irreversible and favorable.

Table 3: Deviations of dye uptake from experimental and theoretical approach for the pseudo-first and pseudo-second-order Kinetic Models with 5 mg/L adsorbate at 303 K.

Adsorbent dose g/L	Removal of dye mg/g (q_e) for first order kinetics			Removal of dye mg/g (q_e) for second order kinetics		
	Theoretical	Experimental	Deviation	Theoretical	Experimental	Deviation
0.1	20.6	44.4	−23.9	47.6	44.4	3.2
0.2	10.6	45.2	−34.6	47.6	45.2	2.4
0.3	9.7	45.9	−36.1	47.6	45.9	1.8
0.4	12.3	46.7	−34.4	47.6	46.7	0.9
0.5	5.2	47.0	−41.8	47.6	47.0	0.6
0.6	5.0	47.4	−42.4	50.0	47.4	2.6
0.7	3.7	48.0	−44.3	50.0	48.0	2.0

3.2.5. Effects of temperature and thermodynamic parameters

Methylene blue dye adsorption by SALP was also carried out for various temperatures (298–328K) with an adsorption time of 120 min

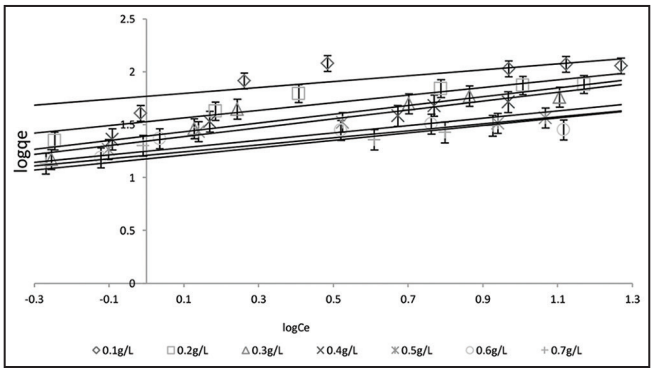

Figure 15: Freundlich isotherm plots for adsorption of methylene blue on *Saraca asoca* leaf powder of different amounts at 303 K for 140 min.

(Figure 17). The van't Hoff plots (Figure 18) of log (q_e/C_e) versus T^{-1} were linear ($r \approx 0.94$) yielding standard adsorption enthalpy range, $\Delta H^0 = -28.84$ to -10.03 kJ/mol. The adsorption was accompanied by decrease in the standard entropy from −0.058 to –−0.013 J/K/mol, suggesting some kind of ordered arrangement of the dye particles on the adsorbent surface compared to their random distribution in aqueous solution.

The standard Gibb's energy at all temperatures (298–328 K) was negative with decreasing trend indicating the adsorption process to be less spontaneous at higher temperature [54]. Table 5 shows ΔH^0 values for different temperatures and the negative values suggested that the adsorption of the cationic dye, methylene blue on SALP was exothermic in nature [55]. ΔS^0 values were also negative indicating the adsorption of the dye particles to be having less randomness at the solid/liquid interface [56]. Furthermore, the initial concentration of the dye solution had shown a trend that ΔH^0 was less negative with increasing concentration of the dye. ΔG^0 was increasing with rising temperature indicating the adsorption to be less at higher temperatures.

Table 4: Parameters of different isotherm models for 5 mg/L methylene blue solution for different doses of *Saraca Asoca* leaf powder.

Parameters	Adsorbent dose (g/L)						
	0.1	**0.2**	**0.3**	**0.4**	**0.5**	**0.6**	**0.7**
Langmuir coefficients							
R^2	0.99	1	0.99	0.98	0.99	0.99	0.98
m	0.01	0.01	0.02	0.02	0.03	0.03	0.03
c	0.01	0.02	0.02	0.02	0.02	0.01	0.03
q_m (mg g^{-1})	125	83.33	66.67	58.82	38.46	30.3	32.26
b (L mg^{-1})	1	0.8	0.71	0.71	1.13	2.36	1.15
R_L	0.01	0.01	0.02	0.02	0.02	0.01	0.03
Freundlich coefficients							
R^2	0.61	0.86	0.83	0.9	0.76	0.63	0.89
m	0.28	0.36	0.41	0.42	0.35	0.33	0.35
c	1.77	1.53	1.39	1.34	1.25	1.21	1.18
n	3.6	2.78	2.43	2.38	2.87	3.03	2.85
1/n	0.28	0.36	0.41	0.42	0.35	0.33	0.35
K_F (L mg^{-1})	58.61	35.65	24.66	22.08	17.74	16.18	15

Table 5: Thermodynamic parameters for adsorption of methylene blue on *Saraca Asoca* leaf powder (0.7 g/L) after an agitation time of 140 min.

Dye (mg/L)	ΔH kJ mol^{-1}	ΔS kJ mol^{-1} K^{-1}	ΔG (kJ mol^{-1}) at temp (K)			
			298	**308**	**318**	**328**
5	−28.84	−0.058	−11.60	−11.02	−10.44	−9.86
10	−18.50	−0.027	−10.50	−10.23	−9.96	−9.69
15	−15.49	−0.019	−9.75	−9.55	−9.36	−9.17
20	−3.21	−0.006	−1.43	−1.37	−1.31	−1.25
25	−14.90	−0.024	−7.85	−7.61	−7.38	−7.14
30	−10.03	−0.013	−6.19	−6.06	−5.93	−5.80

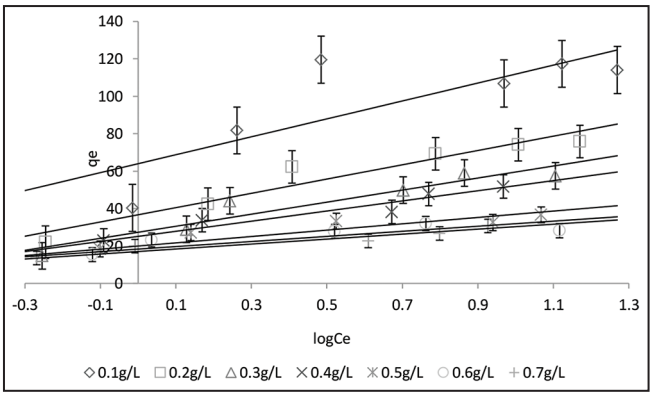

Figure 16: Temkin isotherm plots for adsorption of methylene blue on *Saraca asoca* leaf powder of different amounts at 303 K for 120 min.

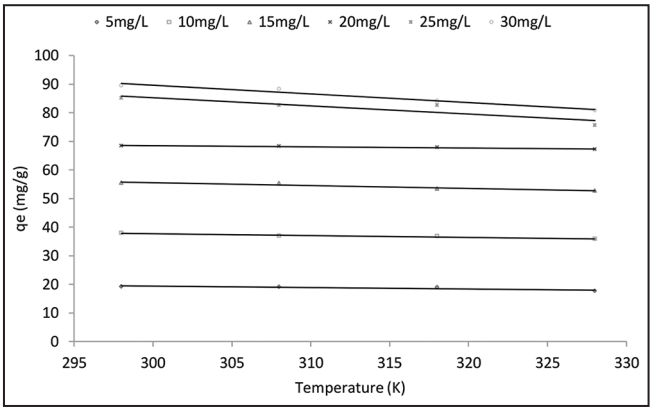

Figure 17: Variation of extent of adsorption (q_e) of methylene dye on *Saraca asoca* leaf powder (0.7 g/L) at 298–328 K for 5–30 mg/L methylene blue (agitation time 120 min).

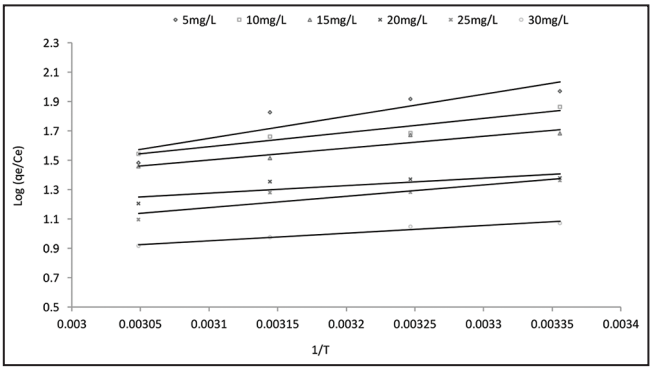

Figure 18: Van't Hoff plots for adsorption of methylene blue on raw *Saraca asoca* leaf powder (0.7 g/L) at 298–328 K with initial concentration 5–30 mg/L of methylene blue (agitation time 120 min).

4. CONCLUSIONS

The bioadsorbent made from the mature leaves of *S. asoca* tree has been found to be an effective material in taking up a cationic dye from its solution. The experimental data fit three traditional isotherms due to Langmuir, Freundlich, and Temkin and the isotherm coefficients point to a favorable process. The adsorption follows pseudo-second-order mechanism and but the intraparticle diffusion does not play a dominant role in the adsorption process. The interactions between the dye molecules and SALP are exothermic accompanied by a decrease in Gibbs energy and entropy. The spontaneity decreases as the temperature increases.

5. REFERENCES

1. M. J. Bhandary, K. R. Chandrasekhar, K. M. Kaveriappa, (1995) Medical ethnobotany of the Siddis of Uttara Kannada district, Karnataka. ***India. Journal of Ethnopharmacology***, 47: 149-58.
2. M. Ali, (2008) ***Pharmacognosy***, New Delhi: CBS Publishers and Distributors, p668-669.
3. T. Viraraghavan, M. M. Dronamraju, (1993) Saraca asoca leaf powder as a biomass-based adsorbent for removal of methylene blue in water, ***Journal of Environmental Health Science Health***, A28: 1261.
4. N. Gupta, A. K. Kushwaha, M. C. Chattopadhyaya, (2012) Adsorption studies of cationic dyes onto Ashoka (Saraca asoca) leaf powder, ***Journal of the Taiwan Institute of Chemical Engineers***, 43: 604-613.
5. S. Chowdhury, K. G. Bhattacharyya, (2019) Use of Cu(II)-incorporated zeolite Y for decolourization of dyes in water: A case study with aqueous methylene blue and Congo red, ***SN Applied Sciences***, 1: 87.
6. A. K. De, (1989) ***Environmental Chemistry***, Meerut: Wiley Eastern Ltd.
7. S. M. S. Arabi, R. S. Lalehloo, M. R. T. Olyai, G. A. M. Ali, H. Sadegh, (2018) Removal of Congo red azo dye from aqueous solution by ZnO nanoparticles loaded on multiwall carbon nanotubes. ***Physica E: Low-dimensional Systems and Nanostructures***, 106: 150-155.
8. H. Sadegh, M. Mazloumbilandi, M. Chahardouri, (2017) Low-cost materials with adsorption performance. In: L. Martínez, O. Khariss-Ova, B. Kharisov, (Eds.), ***Handbook of Ecomaterials***, Berlin, Germany: Springer, p1-33.
9. M. M. Younes, I. I. El-Sharkawy, A. E. Kabeel, B. B. Saha, (2017) A review on adsorbent-adsorbate pairs for cooling applications, ***Applied Thermal Engineering***, 114(5): 394-414.
10. A. Pal, K. Thu, S. Mitra, (2017) Study on biomass derived activated carbons for adsorptive heat pump application, ***International Journal of Heat and Mass Transfer***, 110: 7-19.
11. G. K. Cheruiyot, W. C. Wanyonyi, J. J. Kiplimo, E. N. Maina, (2019) Adsorption of toxic crystal violet dye using coffee husks: Equilibrium, kinetics and thermodynamics study, ***Scientific African***, 5: 2468-2276.
12. C. Sahoo, A. K. Gupta, (2012) Optimization of photocatalytic degradation of methyl blue using silver ion doped titanium dioxide by combination of experimental design and response surface approach, ***The Journal of Hazardous Materials***, 215: 302-310.
13. A. Miclescu, L. Wiklund, (2010) Methylene blue, an old drug with new indications? ***Jurnalul Roman de Anestezie Terapie Intaensiva***, 17: 35-41.
14. V. Tharanitharan, K. Srinivasan, (2009) Studies on the adsorption of Ni(ll) on to modified amberlite XAD-7HP resin, ***Indian Journal of Environmental Protection***, 29: 294-303.
15. S. G. Khosrowshahi, M. A. Behnajady, (2016) Chromium (VI) adsorption from aqueous solution by prepared biochar from Onopordom heteracanthom, ***International Journal of Environmental Science and Technology***, 13: 1803-1814.
16. H. Medhi, K. G. Bhattacharyya, (2017) Kinetic and mechanistic studies on adsorption of Cu(II) in aqueous medium onto montmorillonite K10 and its modified derivative, ***New Journal of***

Chemistry, 41: 13533-13552.
17. M. Witczak, M. Walkowiak, W. Cichy, M. Komorowicz, (2015) The application of elemental analysis for the determination of the elemental composition of lignocellulosic materials, ***Annals of Warsaw University of Life Sciences-SGGW Forestry and Wood Technology***, 92: 477-482.
18. A. Sluiter, B. Hames, R. Ruiz, C. Scarlata, J. Sluiter, D. Templeton, (2005) Determination of Ash in Biomass: Laboratory Analytical Procedure (LAP). In: ***Technical Report: NREL/TP-510-42622, January 2008***. United States of America: National Renewable Energy Laboratory.
19. M. B. Ibrahim, M. S. Sulaiman, S. Sani, (2015) Assessment of Adsorption Properties of Neem Leaves Wastes for the Removal of Congo Red and Methyl Orange. Kuala Lumpur, Malaysia: ***Conference Paper***, ***3rd International Conference on Biological, Chemical and Environmental Sciences*** (***BCES-2015***), Sept. 21-22.
20. S. F. Montanher, E. A. Oliveira, M. C. Rollemberg, (2007) Utilization of agro-residues in the metal ions removal from aqueous solutions, ***The Journal of Hazardous Materials Wastewater Treatment Removal Analysis***, 1: 51-78.
21. M. R. Boniolo, M. Yamaura, R. A. Monteiro, (2010) Biomassa residual para remoção de íonsuranilo, ***Química Nova***, 33: 547-551.
22. R. M. Kostadinova, G. Sikorska, A. E. Navarro, (2014) Acid-base properties of the adsorption of synthetic dyes from solutions, ***Journal of Environmental and Analytical Toxicology***, 4: 240.
23. K. Amel, M. A. Hassena, D. Kerroum, (2012) Isotherm and kinetics study of biosorption of cationic dye onto banana peel, ***Energy Procedia***, 19: 286-295.
24. D. Das, D. P. Sama, B. C. Meikap, (2015) Preparation of activated carbon from green coconut shell and its characterization, ***Journal of Chemical Engineering and Process Technology***, 6: 5.
25. I. J. Idan, L. C. Abdullah, T. S. Y. Choong, S. N. A. Md Jamil, (2018) Equilibrium, kinetics and thermodynamic adsorption studies of acid dyes on adsorbent developed from kenaf core fiber, ***Adsorption Science and Technology***, 36(1-2): 694-712.
26. L. E. Liu, F. Yu, J. Liu, X. Han, H. Zhang, B. Zhang, (2013) Removal of auramine O from aqueous solution using Sesame leaf: Adsorption isotherm and kinetic studies, ***Asian Journal of Chemistry***, 25(4): 1991-1998.
27. A. A. Kamaru, N. S. Sani, N. A. N. Malek, (2016) Raw and surfactant-modified pineapple leaf as adsorbent for removal of methylene blue and methyl orange from aqueous solution, ***Desalination and Water Treatment***, 57(40): 18836-18850.
28. D. J. Shaw, (1980) ***Introduction to Colloid and Surface Chemistry***, London: Butterworth.
29. X. Song, H. Liu, L. Cheng, Y. Qu, (2010) Surface modification of coconut-based activated carbon by liquid-phase oxidation and its effects on lead ion adsorption, ***Desalination***, 255(1-3): 78-83.
30. Y. H. Li, S. Wang, A. Cao, D. Zhao, X. Zhang, C. Xu, Z. Luan, D. Ruan, J. Liang, D. Wu, B. Wei, (2001) Adsorption of fluoride from water by amorphous alumina supported on carbon nanotubes. ***Chemical Physics Letters***, 350(5): 412-416.
31. R. Lafi, I. Montasser, A. Hafiane, (2019) Adsorption of Congo red dye from aqueous solutions by prepared activated carbon with oxygen-containing functional groups and its regeneration, ***Adsorption Science and Technology***, 37(1-2): 160-181.
32. C. T. Weber, E. L. Foletto, L. Meili, (2013) Removal of tannery dye from aqueous solution using papaya seed as an efficient natural biosorbents, ***Water, Air, and Soil Pollution***, 224: 1427-1438.
33. H. Abbasi, H, Asgari, (2018) Removal of methylene blue from aqueous solutions using Luffa adsorbent modified with sodium dodecyl sulfate anionic surfactant, ***Global NEST Journal***, 20(3): 582-588.
34. E. Vunain, D. Kenneth, T. Biswick, (2017) Synthesis and characterization of low-cost activated carbon prepared from Malawian baobab fruit shells by H_3PO_4 activation for removal of Cu (II) ions: Equilibrium and kinetics studies, ***Applied Water Science***, 7: 4301-4319.
35. K. G. Bhattacharyya, A. Sharma, (2005) Kinetics and thermodynamics of methylene blue adsorption on neem (Azadirachta indica) leaf powder, ***Dyes and Pigment***, 65(1): 51-59.
36. H. J. Choi, S. W. Yu, (2019) Biosorption of methylene blue from aqueous solution by agricultural bioadsorbent corncob, ***Environmental Engineering Research***, 24(1): 99-106.
37. S. Kalita, M. Pathak, G. Devi, H. P. Sarma, K. G. Bhattacharyya, A. Sarma, A. Devi, (2017) Utilization of Euryale ferox Salisbury seed shell for removal of basic fuchsin dye from water: Equilibrium and kinetics investigation, ***RSC Advances***, 7: 27248-27259.
38. A. Demirbas, (2003) Trace metal concentrations in ashes from various types of biomass species. ***Energy Sources***, 25(7): 743-751.
39. C. H. Gast, E. Jansen, J. Bierling, L, Haanstra, (1988) Heavy metals in mushrooms and their relationship with soil characteristics, ***Chemosphere***, 17: 789-799.
40. M. Belhachemi, F. Addoun, (2011) Comparative adsorption isotherms and modeling of methylene blue onto activated carbons, ***Applied Water Science***, 1:1 11-117.
41. K. Litefti, M. S. Freire, M. Stitou, J. G. Alvarez, (2019) Adsorption of an anionic dye (Congo red) from aqueous solutions by pine bark, ***Scientific Reports***, 9: 16530.
42. J. O. Amode, J. H. Santos, Z. M. Alam, A. H. Mirza, C. C. Mei, (2016) Adsorption of methylene blue from aqueous solution using untreated and treated (Metroxylon spp.) waste adsorbent: Equilibrium and kinetics studies, ***International Journal of Industrial Chemistry***, 7(3): 333-345.
43. K. S. Padmavathy, G. Madhu, P. V. Haseena, (2016) A study on effects of pH, adsorbent dosage, time, initial concentration and adsorption isotherm study for the removal of hexavalent chromium (Cr (VI)) from wastewater by magnetite nanoparticles, ***Procedia Technology***, 24: 585-594.
44. J. Sarma, A. Sarma, K. G. Bhattacharyya, (2011) Biosorption of Acid Blue 25 on Azadirachta indica (NEEM) Leaf Powder, In: ***World Environmental and Water Resources Congress***, p3927-3940.
45. J. F. Duarte Neto, I. D. S. Pereira, V. C. da Silva, H. C. Ferreira, G. de A. Neves, R. R. Menezes, (2018) Study of equilibrium and kinetic adsorption of rhodamine B onto purified bentonite clays, ***Cerâmica***, 64(372): 598-607.
46. A. S. Franca, L. S. Oliveira, M. E. Ferreira, (2009) Kinetics and equilibrium studies of methylene blue adsorption by spent coffee grounds, ***Desalination***, 249(1): 267-272.
47. N. Ertugay, E. Malkoc, (2014) Adsorption isotherm, kinetic, and thermodynamic studies for methylene blue from aqueous solution by needles of Pinus sylvestris L. Polish Journal of Environmental, 23(6): 1995-2006.
48. G. Annadurai, R. S. Juang, D. J. Lee, (2002) Use of cellulose-based wastes for adsorption of dyes from aqueous solutions, ***The***

Journal of Hazardous Materials, 92(3): 263-274.
49. F. C. Wu, R. L. Tseng, R. S. Juang, (2000) Comparative adsorption of metal and dye on flake-and bead-types of chitosans prepared from fishery wastes, ***The Journal of Hazardous Materials***, 73(1): 63-75.
50. Y. S. Ho, G. McKay, (2003) Sorption of dyes and copper ions onto biosorbents. ***Process Biochemistry***, 38: 1047-1061.
51. G. Mckay, J. F. Porter, G. R. Prasad, (1999) The removal of dye colour from aqueous solutions by adsorption on low-cost materials, ***Water, Air and Soil Pollution***, 114(3-4): 423-438.
52. A. Gurusamy, J. R. Shin, L. D. Jong, (2002) Use of cellulose-based wastes for adsorption of dyes from aqueous solutions, ***The Journal of Hazardous Materials***, 92(3): 263-274.
53. R. B. Arfi, S. Karoui, K. Mougin, A. Ghorbal (2017) Adsorptive removal of cationic and anionic dyes from aqueous solution by utilizing almond shell as bioadsorbent, ***Euro-Mediterranean Journal for Environmental Integration***, 2(1): 1-13.
54. B. Singha, S. K. Das, (2011) Biosorption of Cr (VI) ions from aqueous solutions: Kinetics, equilibrium, thermodynamics and desorption studies, ***Colloids and Surfaces B: Biointerfaces***, 84(1): 221-232.
55. I. E. Ouahabi, R. Slimani, S. Benkaddour, H. Hiyane, N. Rhallabi, B. Cagnon, M. E. Haddad, S. E. Antri, S. Lazar, (2018) Adsorption of textile dye from aqueous solution onto a low cost conch shells, ***Journal of Materials and Environmental Science***, 9(7): 1987-1998.
56. C. Djilani, R. Zaghdoudi, F. Djazi, (2015) Adsorption of dyes on activated carbon prepared from apricot stones and commercial activated carbon, ***Journal of the Taiwan Institute of Chemical Engineers***, 53: 112-121.

****Bibliographical Sketch***

Ms. Jahnabi Deka is a Research Scholar at the Department of Chemistry, Gauhati University, Assam.

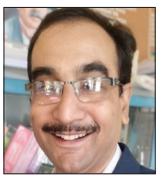

Dr. Hitesh Das is Assistant Professor of Chemistry, M C College, Barpeta, Assam.

Dr. Krishna Gopal Bhattacharyya is Professor of Chemistry, Assam Don Bosco University, Sonapur, Assam.

Professor Krishna Gopal Bhattacharyya retired as Professor of Chemistry, Gauhati University, Assam (India) in 2016. Presently, he is now working as Professor of Chemistry, Assam Don Bosco University. More than 70 students have completed their Ph D under his guidance. His research interests include air, water and soil chemistry, Heterogeneous Catalysis and Environmental Chemistry. He has more than 200 research publications in international and national journals with > 11000 citations and a h-index of 44 and i10 index of 87. He had research projects from World Bank, DST, DBT, Ministry of Environment and Forests, ISRO, DRDO and other organizations. In a recent study by Ioannidis JPA, Boyack KW, Baas J (2020) of Stanford University (USA) on top 2% Scientists worldwide in various fields, Prof. K G Bhattacharyya has been ranked third among top Indian Scientists and 235th among World Scientists in the field of 'Environmental Science'.